

Epitaxy of Au on Ag(111) Studied by High-Energy Ion Scattering

R. J. Culbertson,^(a) L. C. Feldman, and P. J. Silverman
Bell Laboratories, Murray Hill, New Jersey 07974

and

H. Boehm^(b)
Rutgers University, New Brunswick, New Jersey 08903

(Received 27 April 1981)

The first stage of epitaxial growth of Au on Ag(111) has been studied by MeV ion scattering. The monolayer-by-monolayer (Frank-van der Merwe) growth mode for this system is confirmed by measurements of (1) the Ag surface peak, (2) the Au-Au shadowing effect, and (3) the Ag Auger intensity.

PACS numbers: 68.55.+b, 68.48.+f, 79.20.Fv

Epitaxial growth of thin films has been divided into three categories: (1) the Volmer-Weber mode, in which the surface energy of the film material is large compared with that of the substrate, i.e., Au on NaCl; (2) the Frank-van der Merwe mode in which the surface energy of the film is less than or comparable to that of the substrate and there is low strain energy in the film, and (3) the Stranski-Krastanov mode in which the surface energy of the film is less than or comparable to that of the substrate but there is a high strain energy in the film.¹ The Frank-van der Merwe mode is characterized as layer-by-layer growth (as opposed to three-dimensional island formation) and is generally applicable in cases of autoepitaxy (i.e., Si on Si) or in cases of "almost autoepitaxy" (i.e., metal *A* on metal *B* with a close match in lattice constant). The initial stages of growth in this mode are necessarily studied by the surface-science techniques of low- or medium-energy electron diffraction (LEED or MEED) and Auger analysis.

In this Letter we describe the first systematic study of Au epitaxial growth on a Ag(111) surface using high-energy ion scattering. We show that the growth mode in this system is clearly of a Frank-van der Merwe type (as expected) and that ion scattering techniques are particularly suited to these studies.

Experiments were carried out in an UHV system equipped with LEED and Auger apparatus and a Au deposition source.² The UHV system is directly coupled to a Van de Graaf accelerator so that high-energy ion scattering experiments can be performed *in situ*. Prior to Au deposition, the bulk Ag(111) samples were cleaned via sputtering and annealing. They showed essentially no trace impurities either in the Auger scan or in the ion scattering spectra; the LEED pattern displayed

a sharp, well-defined (1×1) pattern. The magnitude of the surface peak in the normal $\langle 111 \rangle$ direction and the off-normal $\langle 110 \rangle$ direction was in good agreement with calculations assuming a "bulklike" surface. Analyses of this data indicated that both horizontal and vertical displacements of the surface atoms in the clean Ag surface are $< 0.1 \text{ \AA}$, in good agreement with LEED analyses.³ Au deposition was monitored primarily through the ion scattering spectra, although Auger spectra were checked following Au deposition to affirm that light impurity contamination was negligible. Measurements and evaporation were done with the substrate at room temperature and at 140°K .

The first indication of epitaxy in the scattering experiments is the reduction of the substrate surface peak (SP).⁴ For a clean crystal the SP results from the interaction of the aligned ion beam with the first monolayer(s) of the single crystal solid. The first atom in an ideal string of atoms parallel to the beam forms a shadow cone which reduces the probability of close encounters between incident ions and atoms further along the string. There is always an interaction with the first atom (monolayer) and subsequent interactions depend on the ratio of the vibrational amplitude of the atoms to the shadow-cone radius.⁵ Ideal epitaxial overlayers of different atomic species shadow the beam from the first substrate atoms and reduce the substrate SP. It is well established that ion scattering and channeling is a probe of crystalline order on the submicron scale, i.e., as in annealing studies and epitaxial film investigations. Analysis of the SP tests for crystallinity (order) on the monolayer scale. The main point of this paper is to illustrate the use of SP analysis in studies of epitaxial growth.

The overlayer shadowing effect is illustrated in

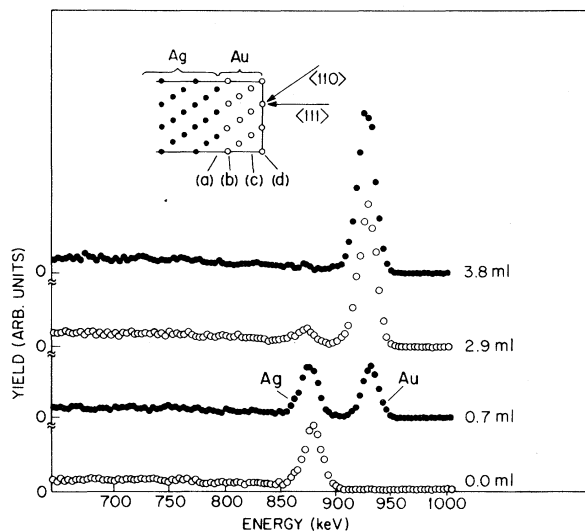


FIG. 1. Room-temperature backscattering spectra for 1.0-MeV He⁺ incident along the <011> direction of (a) clean Ag, (b) Ag+0.7 ml of Au, (c) Ag+2.9 ml of Au, and (d) Ag+3.8 ml of Au. The inset schematically indicates the overlayer thickness for each of these cases.

Fig. 1 for 1.0-MeV He⁺ incident on the clean and Au-covered surface of Ag(111) in the <110> crystal direction. The clean Ag spectra show the expected Ag SP and a low-energy distribution corresponding to scattering from the bulk. The intensity of the Ag SP is close to that expected from the systematics and theoretical prediction of this quantity.⁵ The Au-covered surfaces show the dramatic decrease of the Ag SP as a result of Au shadowing. Per Au monolayer the shadowing is more complete in the <110> direction than in the

<111> direction. As shown in the inset of Fig. 1 this is a result of the geometry of the fcc surface; three monolayers of Au just cover all the Ag rows as viewed in the <111> direction but triply cover all the Ag rows as viewed in the <110> direction. Note that the SP reduction in the <110> direction is evidence that the Au spacing in the vertical direction is a close match to the Ag spacing (within $\leq 0.1 \text{ \AA}$) while the reduction in the normal <111> direction (not shown) indicates a close match in atomic spacing in the surface plane.

As coverage is increased to beyond one monolayer there is a possibility of Au-Au shadowing. That is, the surface epitaxial layer(s) shadow the underlying adsorbate layer(s) from the beam. This effect is easily measured by determining the ratio of the Au scattering yield in the aligned direction to that in the nonaligned direction. By analogy to channeling experiments this quantity is referred to as $\chi_{\text{min}}(\text{Au})$. The dependence of $\chi_{\text{min}}(\text{Au})$ on coverage distinguishes the different epitaxial growth modes mentioned above. In Frank-van der Merwe growth there is no Au-Au shadowing [$\chi_{\text{min}}(\text{Au})=1.0$] prior to the completion of one monolayer. For higher coverage $\chi_{\text{min}}(\text{Au})$ would decrease in a predictable fashion. On the other hand, island formation would result in $\chi_{\text{min}}(\text{Au}) < 1$ for average coverage less than one monolayer. While the rate of decrease of the Ag surface peak is also sensitive to the growth mode we have found $\chi_{\text{min}}(\text{Au})$ more easily measurable and more directly interpretable.

Figure 2 shows the dependence of the Ag SP and $\chi_{\text{min}}(\text{Au})$ as a function of Au coverage for growth and analysis at 140°K. The abscissa is derived

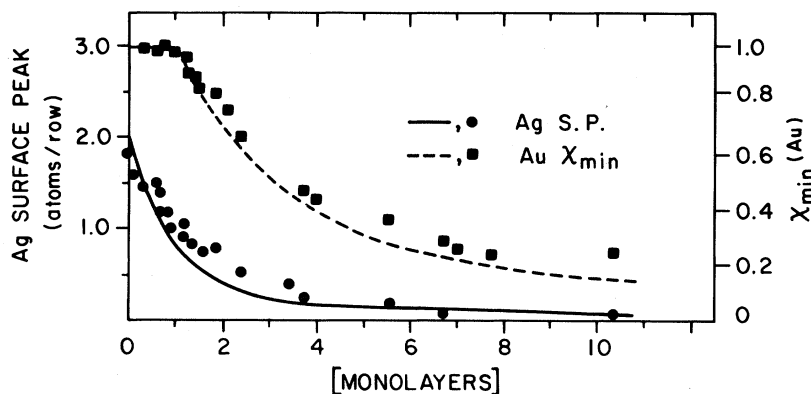


FIG. 2. Ag surface-peak yield and $\chi_{\text{min}}(\text{Au})$ at 140°K as a function of Au coverage for 1.0-MeV He⁺ incident along the <011> direction. The full curve and dashed curve are derived from computer simulations assuming monolayer-by-monolayer growth.

from Rutherford backscattering which yields the coverage in Au atoms/cm² with an accuracy of $\pm 5\%$. The number is then converted to monolayers for ease of comparison with different coverage models. The curves in Fig. 2 are derived from computer simulations of the scattering process.^{5,6} The simulations assume bulk, uncorrelated vibrational amplitudes for atoms in both the Au film and the Ag substrate. Furthermore, a monolayer-by-monolayer growth process is assumed. Other islanding or random-coverage models would predict a different dependence for both $\chi_{\min}(\text{Au})$ and Ag SP. Similar results were obtained from experiments and calculations at 300 °K.

The shape of the $\chi_{\min}(\text{Au})$ data corresponds to the Frank-van der Merwe growth mode; that is $\chi_{\min}(\text{Au})=1.0$ for Au coverage up to one monolayer and then is reduced in a predictable fashion. The prediction of the dependence of the Ag SP on Au coverage also follows the general trend of the data. Note that both types of data shown in Fig. 2 are important: $\chi_{\min}(\text{Au})$ measures the quality of the grown layer and the Ag SP measures the registry of the overlayer to the substrate.

Bulk diffusion of Au into the single-crystal Ag substrate is expected to be negligible at or below room temperature.^{7,8} The present results indicate that inward diffusion of Au at the Ag surface is also negligible at or below room temperature on the *monolayer* scale. Heating the Au on Ag sample above 350 °C for a few tens of minutes resulted in significant interdiffusion as determined by both high-energy ion scattering and Auger analysis.

In general, growth mechanisms can also be distinguished by analysis of the substrate Auger signal as a function of overlayer thickness.⁹ We have carried out such an analysis for the Au on Ag(111) system as shown in Fig. 3. The abscissa is determined by the Rutherford backscattering yield. The 351–356-eV Ag Auger intensity is well fitted by an exponential curve with a decay length of 6.0 Å. Monolayer-by-monolayer growth is well approximated by an exponential curve, and the decay length derived from the data is in good agreement with the systematics of electron escape lengths.¹⁰ We feel that this measurement is particularly accurate since both the areal density and the uniformity of the overlayer are well established. The good fit by a simple exponential decay again supports the monolayer-by-monolayer growth mode. Further details of the growth mechanism were established by analysis of the

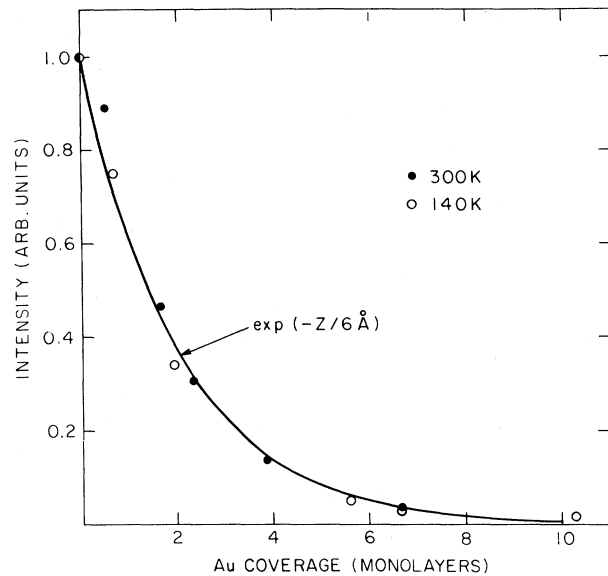


FIG. 3. Relative Ag (351–356 eV) Auger yield as a function of Au coverage. The coverages were accurately derived from Rutherford backscattering measurements of areal density. The good agreement between the experimental values and the calculations justifies labeling the abscissa in true monolayers.

energy dependence of the LEED pattern for Au coverage of a fraction of a monolayer. The periodic dependence of the breadth of the specular beam as a function of incident energy was consistent with islands with a step height equal to that of the bulk atomic spacing. The ion scattering results require that these islands be one-monolayer high.

The ion scattering measurements reveal another feature of the grown layers, namely, that the Au coverage is primarily in the fcc sequence. Gold atoms in the first monolayer occupying hexagonal sites would not shadow the Ag along the $\langle 110 \rangle$ direction. The good agreement between the calculated and experimental suppression of the Ag surface peak (Fig. 2) places an upper limit of $\sim 10\%$ on Au atoms in hexagonal sites. This is in agreement with the LEED results of Soria and Sacedon, who also studied the Au on Ag(111) system.⁷

We have illustrated the use of basic ion scattering parameters, supplemented by LEED and Auger analysis, to monitor the first stages of epitaxial growth. The suppression of the substrate surface peak is a measure of registry of the overlayer to the substrate, and the suppression of scattering within the overlayer in the channeling direction [$\chi_{\min}(\text{overlayer})$] is a meas-

ure of crystal quality in the epitaxial film. In the case of Au epitaxial formation on Ag(111) the growth is clearly shown to be by a Frank-van der Merwe mechanism. With these techniques we have been able to monitor the deposition of alternate layers of Au and Ag (a few monolayers at a time), observing the suppression of the surface peak of the underlying material as a measure of lattice registry. The high-energy ion scattering technique will be an important addition in studying epitaxial growth and superlattices.

We wish to acknowledge W. F. Flood for preparing the Ag samples.

^(a)Present address: Solid State Division, Oak Ridge National Laboratory, Oak Ridge, Tenn. 37838.

^(b)Present address: Riesterstrasse 22, A-4050 Traun, Austria.

¹J. A. Venables and G. L. Price, in *Epitaxial Growth*, edited by J. W. Mathews (Academic, New York, 1975), part B.

²L. C. Feldman, P. J. Silverman, and I. Stensgaard, Nucl. Instrum. Methods **168**, 589 (1980).

³F. Soria, J. L. Sacedon, P. M. Echenique, and D. Titterington, Surf. Sci. **68**, 448 (1977).

⁴E. Bøgh, in *Channeling*, edited by D. V. Morgan (Wiley, London, 1973).

⁵I. Stensgaard, L. C. Feldman, and P. J. Silverman, Surf. Sci. **77**, 513 (1978).

⁶H. J. Boehm, master's thesis, Rutgers University, 1980 (unpublished).

⁷F. Soria and J. L. Sacedon, Thin Solid Films **60**, 113 (1979).

⁸H. E. Cook and J. E. Hilliard, J. Appl. Phys. **40**, 2191 (1969).

⁹P. W. Palmberg and T. N. Rhodin, J. Appl. Phys. **39**, 2425 (1968).

¹⁰C. J. Powell, Surf. Sci. **44**, 29 (1974).

Phonon Focusing of Large- \vec{k} Acoustic Phonons in Germanium

W. Dietsche, G. A. Northrop, and J. P. Wolfe

Physics Department and Materials Research Laboratory, University of Illinois at Urbana-Champaign, Urbana, Illinois 61801

(Received 1 June 1981)

Combining heat-pulse scanning and tunnel-junction detection, we have observed ballistic propagation of high frequency (>700 GHz) acoustic phonons over ~ 1 -mm path lengths in germanium. The ballistic nature of the phonons is determined by sharp variations in phonon flux with propagation angle. The phonon focusing pattern is significantly altered from that obtained with an Al bolometer (which is sensitive to longer-wavelength phonons) revealing a modification of the phonon slowness surface due to dispersion.

PACS numbers: 66.70.+f, 63.20.Dj

Over the last few years there has been a continuous effort to develop techniques for observing the ballistic propagation of phonons of ever higher frequencies over macroscopic distances.¹ Such propagation of phonons with \vec{k} approaching the Brillouin-zone edge and frequencies about 1 THz has now been reported by several groups.²⁻⁵ Large- \vec{k} acoustic phonons are of particular interest because of their dispersive nature and their applicability to high-frequency phonon spectroscopy. Fundamental questions remain concerning the lifetime and mean free path of such phonons. In this Letter we report experiments which display the anisotropic propagation of large- \vec{k} phonons in Ge. The ballistic phonon imaging method

we describe is a general method which shows promise for producing a global picture of the acoustic-phonon dispersion in a crystal.

High-frequency phonons can be produced by a number of means, including thin-film heaters, superconducting tunnel junctions, far-infrared lasers, and hot-carrier relaxation in a semiconductor. Our experiments use this last method, with the hot carriers being photoproduced by a pulsed laser. The carrier relaxation in this case produces a broad distribution of phonon frequencies in the 1-THz range. If the ambient crystal temperature is low enough ($T \lesssim 10$ K), the mean free path of near-THz phonons should be limited by impurity, defect, or isotope scattering. In